Journal of Materials Chemistry

www.rsc.org/materials

Volume 21 | Number 21 | 7 June 2011 | Pages 7489–7828

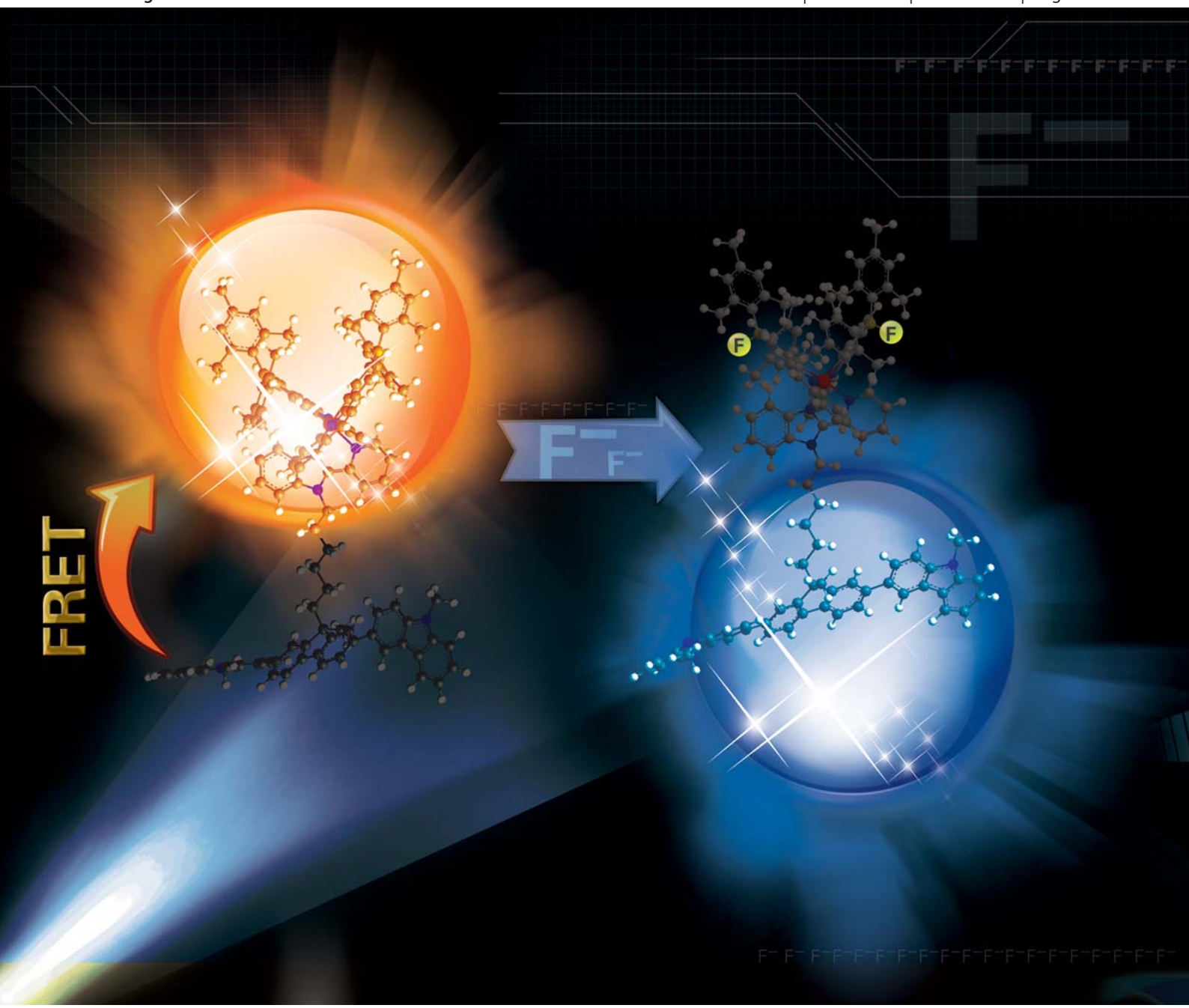

ISSN 0959-9428

RSC Publishing

PAPER

Wei Huang *et al.*

FRET-based probe for fluoride based on a phosphorescent iridium(III) complex containing triarylboron groups

Journal of Materials Chemistry

Dynamic Article Links

Cite this: J. Mater. Chem., 2011, 21, 7572

www.rsc.org/materials

PAPER

Published on 24 March 2011. Downloaded by Nipissing University on 17/10/2014 03:02:48.

FRET-based probe for fluoride based on a phosphorescent iridium(III) complex containing triarylboron groups†

Wenjuan Xu, Shujuan Liu, Huibin Sun, Xinyan Zhao, Qiang Zhao,* Shi Sun, Shan Cheng, Tingchun Ma, Lixia Zhou and Wei Huang*

Received 6th January 2011, Accepted 28th February 2011
DOI: 10.1039/c1jm00071c

An excellent F^- probe (complex **1**) based on carbazole-fluorene-carbazole (CzFCz) as a fluorescent donor and a cationic Ir(III) complex unit containing dimesitylboryl (Mes_2B) groups as a phosphorescent acceptor has been designed and synthesized. Several reference compounds, such as complex **2** which is similar to complex **1** but without Mes_2B groups, fluorescent donor CzFCz, and phosphorescent acceptors **A1** and **A2**, were also synthesized in order to better understand the influence of Mes_2B groups on the excited state properties and fluorescence resonance energy transfer (FRET) in this system. The introduction of Mes_2B groups on the ligands of the Ir(III) complex unit can lead to a red-shifted and more intense absorption, facilitating efficient FRET from the fluorescent donor to the phosphorescent acceptor. Complex **1** displayed highly efficient orange-red phosphorescent emission with an emission peak at 584 nm in CH_2Cl_2 solution at room temperature. The emission wavelength of complex **1** in film is red-shifted to 600 nm with a shoulder at 650 nm, and its quantum efficiency in film was measured to be 0.15 under excitation at 450 nm. Utilizing the specific Lewis acid–base interactions between boron atom and F^-, the binding of F^- to complex **1** can change its excited state and suppress FRET, quenching the phosphorescent emission from the Ir(III) complex and enhancing the fluorescent emission from CzFCz. Thus, a visual change in the emission color from orange-red to blue was observed. Optical responses of complex **1** to F^- revealed that it can be used as a highly selective, colorimetric and ratiometric optical probe for F^- utilizing the switchable phosphorescence and fluorescence.

Introduction

As we all know, fluoride (F^-) is an important microelement in the human body.[1] Water fluoridation or addition of fluoride to toothpaste has become a widespread practice because of the beneficial effects of this anion in dental health. High doses of this anion are, however, dangerous and can lead to dental or skeletal fluorosis. Due to the possible toxicity of this anion, the design of fluorescent F^- probes is an area of active investigation, and a great deal of effort has been devoted to the design of molecular receptors containing binding sites to F^-.[2] Original efforts focused on receptors that interact with F^- *via* hydrogen bonds,[3] but the selectivity is often not good. Recently, specific Lewis acid–base interactions, such as the strong affinity of a boron atom toward F^-, have been adopted as an efficient approach for fluoride detection.[4] Some three-coordinated boron compounds with a donor–π conjugation–acceptor (D–π–A) chemical structure, in which the dimesitylboryl (Mes_2B) group was adopted as the electron acceptor and receptor for F^-, were reported to be highly selective fluorescent probes for F^-. In the presence of F^-, the strong B–F^- interaction can interrupt the extended π conjugation of these organoboron derivatives, thereby causing a dramatic change in the photophysical properties.

Currently, organic luminophores are widely used as fluorescent probes. In addition to purely organic luminophores, most recently, the use of phosphorescent heavy-metal complexes as probes has also attracted considerable interest,[5] as a result of their advantageous photophysical properties, such as sensitivity of emission properties to the changes of local environment, evident Stokes shifts for easy separation of excitation and emission, significant single-photon excitation in the visible range and relatively long lifetimes (from the order of microseconds to milliseconds) compared to those of purely organic luminophores. In addition, compared with purely organic luminophores, the excited-state properties of phosphorescent heavy-metal complexes are more complicated and depend on the metal centers, chemical structures and triplet state energy levels of the

Key Laboratory for Organic Electronics & Information Displays (KLOEID) and Institute of Advanced Materials (IAM), Nanjing University of Posts and Telecommunications, Nanjing, 210046, P. R. China. E-mail: wei-huang@njupt.edu.cn; iamqzhao@njupt.edu.cn; Fax: +86 25 8586 6008; Tel: +86 25 8586 6008

† Electronic supplementary information (ESI) available: Graphs showing response of UV-vis absorption spectra of **1** to various anions (Fig. S1) and response of PL spectra of **1** to various anions (Fig. S2), and the calculation of F^- binding constant from the UV-vis titration data (Fig. S3). See DOI: 10.1039/c1jm00071c

This journal is © The Royal Society of Chemistry 2011

Published on 24 March 2011. Downloaded by Nipissing University on 17/10/2014 03:02:48.

ligands. If a heavy-metal complex contains a specific binding site in its ligand for an analyte, the presence of this analyte can lead to dramatic variations in its photophysical and excited state properties, realizing the detection. According to this principle, we have successfully realized excellent phosphorescent probes for Hg^{2+}, anions and homocysteine based on Ir(III) complexes.[6]

Introducing Mes_2B groups into the ligands of phosphorescent heavy-metal complexes can realize phosphorescent F^- detection through the specific interaction of a boron atom with F^-, which can induce variations in the excited state properties of heavy-metal complexes. Most recently, several phosphorescent probes for F^- based on heavy-metal complexes containing a Mes_2B group have been reported by us and other groups.[6c,e,7] Considering their rich photophysical properties and excellent sensing ability, it is necessary to further exploit this class of interesting phosphorescent probes, especially ratiometric probes. The ratiometric detection can increase the sensitivity by measuring the ratio changes of the fluorescence intensities at two different wavelengths, and minimize the external and environment influences.[8] In order to realize the ratiometric F^- probes based on phosphorescent heavy-metal complexes, there are often two approaches adopted. The first approach is to attach a Mes_2B group onto an appropriate position of a complex in which there are dual signaling pathways, and the B–F^- binding can change the excited state properties of the complexes and induce the interconversion between the two signaling pathways, realizing the ratiometric detection of F^-.[7e] Secondly, if there is no dual signaling pathway for the heavy-metal complexes and the interaction of the boron atom with F^- possibly quenches the phosphorescent emission, a donor–acceptor (D–A) structure is usually adopted. Effective ratiometric detection can be realized through the variation of fluorescent resonance energy transfer (FRET) induced by F^- which determines the emission intensity of D and A. For this approach, the linking between D and A can be conjugated (Fig. 1a) or nonconjugated (Fig. 1b). As for the conjugated linking, the energy donor acts as the ligand of the heavy-metal complex (A) and participates in the excited state of the complex (see Fig. 1a). However, for the nonconjugated linking, the heavy-metal complex is tethered to the energy donor with an alkyl chain (Fig. 1b). Thus, the donor has no significant influence on the excited state of the complex. For both kinds of probes, in the absence of F^-, the FRET is efficient and strong phosphorescence from the complex is observed. Binding to F^- may change the excited state of the complex and suppress FRET, quenching the phosphorescent emission from A and enhancing the fluorescent emission from D. Thus, the ratiometric detection

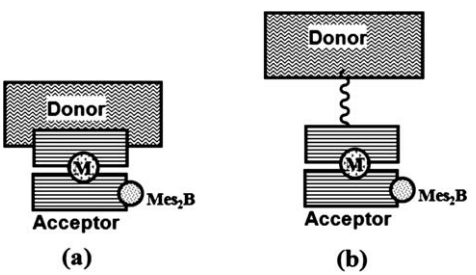

Fig. 1 Phosphorescent F^- probes based on heavy-metal complexes containing a Mes_2B group with conjugated (a) and nonconjugated (b) donor–acceptor structures.

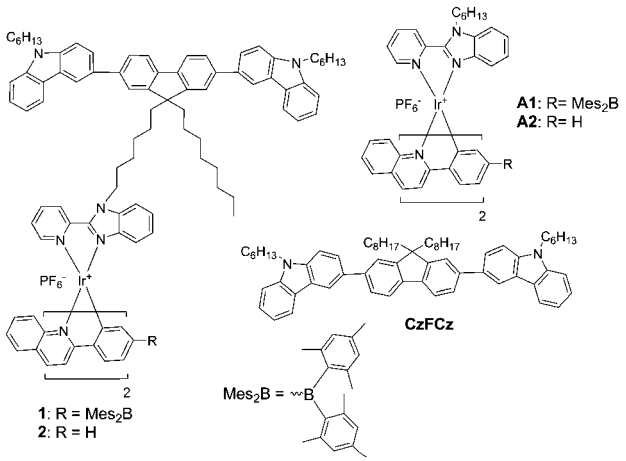

Scheme 1 Chemical structures of compounds synthesized in this work.

of F^- can be realized. Most recently, we have reported a ratiometric F^- probe based on an Ir(III) complex with conjugated D–A structure as shown in Fig. 1a.[6e] In this work, we paid attention to exploitation of an excellent ratiometric F^- probe based on an Ir(III) complex with nonconjugated D–A structure as shown in Fig. 1b, and further investigated the effect of B–F^- binding on the energy transfer from donor to acceptor.

Herein, we synthesized a complex **1** based on carbazole-fluorene-carbazole (CzFCz) as the fluorescent donor and a Mes_2B group-functionalized cationic Ir(III) complex as the phosphorescent acceptor (see Scheme 1). In addition, several reference compounds (shown in Scheme 1), such as complex **2** without Mes_2B groups, fluorescent donor CzFCz, and phosphorescent acceptors **A1** and **A2**, were also synthesized in order to better understand the influence of Mes_2B groups on the excited state properties and FRET of the complex. Finally, the binding of F^- to complex **1** changes the excited state properties of the phosphorescent acceptor, inducing variation in FRET from donor to acceptor, and realizes an excellent colorimetric and ratiometric probe for F^- with switchable phosphorescence and fluorescence signals.

Experimental section

Characterization

NMR spectra were recorded on a Bruker Ultra Shield Plus 400 MHz NMR instrument (^{1}H: 400 MHz, ^{13}C: 100 MHz). Mass spectra were obtained on a Bruker autoflex MALDI-TOF/TOF mass spectrometer and Thermo Scientific ESI-MS spectrometer. The UV-visible absorption spectra were recorded on a Shimadzu UV-3600 UV-VIS-NIR spectrophotometer. Photoluminescent spectra were measured using a RF-5301PC spectrofluorophotometer. The quantum efficiency for **1** was measured in degassed CH_2Cl_2 using *fac*-Ir(ppy)$_3$ (*fac*-tris(2-phenylpyridine)iridium) as the standard.

Computational details

The calculation was performed using the Gaussian 03 suite of programs.[9] The optimizations of complex structures were performed using B3LYP density functional theory (DFT). The LANL2DZ basis set was used to treat the iridium atom, whereas

Published on 24 March 2011. Downloaded by Nipissing University on 17/10/2014 03:02:48.

the 6-31G* basis set was used to treat all other atoms. The contours of the highest occupied molecular orbitals and lowest unoccupied molecular orbitals (HOMOs and LUMOs) were plotted.

Materials

All reagents, unless otherwise specified, were obtained from Sigma-Aldrich, Acros, and Alfa and used as received. All solvents were purified before use. All reactions were performed under nitrogen atmosphere.

Synthesis

9-Hexyl-carbazol-3-boronic acid, 2-(4-bromophenyl)quinoline (Brpq), 2-(4-(dimesitylboryl)phenyl)quinoline (Bpq), and 2,7-dibromo-9-octyl-9*H*-fluorene were prepared according to the literature procedures.[10–12]

1-Hexyl-2-(pyridin-2-yl)-1*H*-benzo[*d*]imidazole (Pbi-C_6)[13]. KOH (0.28 g, 5.1 mmol) and 2-(2-pyridyl)benzimidazole (0.50 g, 2.55 mmol) were added to ionic liquid (20 mL), and the mixture was stirred magnetically for 5 min. Then, 1-bromohexane (0.7 mL, 5.1 mmol) was introduced in a single portion, the stirring was continued for 5 h. After the reaction was complete, the product was extracted with Et_2O (3 × 5 mL). The combined ethereal phases were evaporated under reduced pressure, and the crude product was purified by column chromatography on silica by using ethyl acetate/petroleum ether (1 : 3) as eluent to yield colorless oil product (0.46 g, 65%). ^{1}H NMR (400 MHz, $CDCl_3$, 298 K): δ = 8.68 (d, J = 4.0 Hz, 1H), 8.39 (d, J = 8.0 Hz, 1H), 7.86–7.82 (m, 2H), 7.45 (dd, J = 6.7, 2.0 Hz, 1H), 7.36–7.28 (m, 3H), 4.82 (t, J = 8.0 Hz, 3H), 1.87 (dt, J = 15.0 Hz, 7.6 Hz, 2H), 1.37–1.25 (m, 6H), 0.85 (t, J = 7.1 Hz, 3H); ^{13}C NMR (100 MHz, $CDCl_3$, 298 K): δ = 150.93, 150.08, 148.76, 142.80, 136.89, 136.78, 124.82, 123.80, 123.32, 122.60, 120.22, 110.37, 45.58, 31.46, 30.13, 26.62, 22.64, 14.12.

1-(6-Bromohexyl)-2-(pyridin-2-yl)-1*H*-benzo[*d*]imidazole (Br-pbi)[13]. KOH (2.86 g, 51 mmol) and 2-(2-pyridyl)benzimidazole (2 g, 10.2 mmol) were added to ionic liquid (20 mL), and the mixture was stirred magnetically for 5 min. Then, 1,6-dibromohexane (8 mL, 51 mmol) was introduced in a single portion, the stirring was continued for 5 h. After the reaction was complete, the product was extracted with Et_2O (3 × 20 mL). The combined ethereal phases were evaporated under reduced pressure, and the crude product was purified by column chromatography on silica by using ethyl acetate/petroleum ether (1 : 3) as eluent to yield colorless oil product (2.2 g, 60%). ^{1}H NMR (400 MHz, $CDCl_3$, 298 K): δ = 8.70 (d, J = 4.80 Hz, 1H), 8.41 (d, J = 7.97 Hz, 1H), 7.88–7.33 (m, 2H), 7.46–7.44 (m, 1H), 7.37–7.30 (m, 3H), 4.84 (t, J = 7.6 Hz, 2H), 3.38 (t, J = 6.8 Hz, 2H), 1.95–1.88 (m, 2H), 1.86–1.79 (m, 2H), 1.53–1.44 (m, 2H), 1.42–1.35 (m, 2H); ^{13}C (100 MHz, $CDCl_3$, 298 K): δ = 150.79, 149.94, 148.76, 142.71, 136.94, 136.69, 124.82, 123.88, 123.40, 122.68, 120.23, 110.28, 45.36, 33.88, 32.64, 29.94, 27.81, 26.07.

1-(6-(2,7-Dibromo-9-octyl-fluoren-9-yl)hexyl)-2-(pyridin-2-yl) benzoimidazole (BrfpbiBr). Br-pbi (1.4 g, 4.0 mmol), 2,7-dibromo-9-octyl-9*H*-fluorene (4.0 mmol) and KOH (20 mmol) were added to DMSO (10 mL). The solution was stirred at 60 °C for 5 h. After the reaction was complete, the mixture was poured into H_2O (40 mL), and then was extracted three times with ethyl acetate. The combined organic layers were washed with brine and dried over anhydrous $MgSO_4$. The solvent was removed under reduced pressure. The crude product was purified by column chromatography on silica by using ethyl acetate/petroleum ether (1 : 3) as eluent to yield a white solid (74%). ^{1}H NMR (400 MHz, $CDCl_3$, 298 K): δ = 8.61 (d, J = 4.59 Hz, 1H), 8.36 (d, J = 7.92 Hz, 1H), 7.85–7.80 (m, 2H), 7.52–7.29 (m, 10H), 4.73 (t, J = 7.38 Hz, 2H), 1.90–1.84 (m, 4H), 1.74–1.67 (m, 2H), 1.25–1.04 (m, 14H), 0.83 (t, J = 6.97 Hz, 3H), 0.6–0.49 (m, 4H); ^{13}C NMR (100 MHz, $CDCl_3$, 298 K): δ = 152.48, 150.81, 149.96, 148.70, 142.72, 139.16, 136.86, 136.67, 130.33, 126.20, 124.76, 123.77, 123.32, 122.58, 121.61, 121.31, 120.17, 110.30, 55.70, 45.34, 40.30, 40.17, 31.88, 30.03, 29.95, 29.27, 26.52, 23.69, 22.72, 14.21.

CzfpbiCz. To a mixture of BrfpbiBr (0.71 g, 1 mmol), 9-hexyl-carbazol-3-boronic acid (0.62 g, 2.1 mmol), and $Pd(PPh_3)_4$ (0.006 g, 0.005 mmol), a degassed mixture of toluene, aqueous 2 M potassium carbonate and ethanol (2 : 1 : 1 in volume) 3 mL was added. The mixture was vigorously stirred at 70 °C for 24 h. After the mixture was cooled to room temperature, it was washed with brine, extracted three times with CH_2Cl_2, dried over anhydrous Na_2SO_4. The solution was concentrated. The crude product was purified by column chromatography on silica by using ethyl acetate/petroleum ether (1 : 3) as eluent to yield a white solid (0.63 g, 60%). ^{1}H NMR (400 MHz, $CDCl_3$, 298 K): δ = 8.54 (d, J = 4.37 Hz, 1H), 8.39 (d, J = 1.26 Hz, 2H), 8.19 (d, J = 7.70 Hz, 2H), 7.83–7.78 (m, 5H), 7.73–7.67 (m, 5H), 7.55–7.39 (m, 7H), 7.74–7.17 (m, 6H), 4.67 (t, J = 7.70 Hz, 2H), 4.35 (t, J = 7.13 Hz, 4H), 1.95–1.88 (m, 4H), 1.75–1.66 (m, 2H), 1.53–1.44 (m, 2H), 1.52–1.35 (m, 2H), 1.46–1.28 (m, 16H), 1.21–1.11 (m, 14H), 0.88 (t, J = 6.91 Hz, 9H); ^{13}C NMR (100 MHz, $CDCl_3$, 298 K): δ = 151.62, 148.75, 141.06, 141.00, 139.58, 136.84, 132.87, 128.65, 127.93, 126.95, 126.30, 126.33, 125.94, 125.39, 124.79, 123.84, 123.52, 123.40, 123.11, 121.70, 120.61, 120.04, 119.94, 119.01, 118.92, 110.38, 109.05, 108.99, 55.35, 45.46, 43.39, 40.77, 40.66, 32.07, 31.97, 31.76, 30.22, 30.07, 29.85, 29.81, 29.51, 29.42, 29.38, 29.15, 27.15, 26.63, 22.84, 22.75, 22.71, 14.28, 14.22, 14.19.

CzFCz. To a mixture of 2,7-dibromo-9,9-dioctyl-fluorene (0.55 g, 1 mmol), 9-hexyl-carbazol-3-boronic acid (0.62 g, 2.1 mmol), and $Pd(PPh_3)_4$ (0.006 g, 0.005 mmol), a degassed mixture of toluene, aqueous 2 M potassium carbonate and ethanol (2 : 1 : 1 in volume) 3 mL was added. The mixture was vigorously stirred at 70 °C for 24 h. After the mixture was cooled to room temperature, it was washed with brine, extracted three times with CH_2Cl_2, dried over anhydrous Na_2SO_4. The solution was concentrated. The crude product was purified by column chromatography on silica by using ethyl acetate/petroleum ether (1 : 3) as eluent to yield a white solid (0.62 g, 70%).^{1}H NMR (400 MHz, $CDCl_3$, 298 K): δ = 8.40 (d, J = 1.6 Hz, 1H), 8.21 (d, J = 7.7 Hz, 1H), 7.84–7.80 (m, 4H), 7.73–7.70 (m, 4H), 7.52–7.43 (m, 6H), 7.29–7.25 (m, 2H), 4.35 (t, J = 7.2 Hz, 4H), 2.14–2.10 (m, 4H), 1.96–1.88 (m, 4H), 0.89 (t, J = 7.1 Hz, 6H), 0.79 (t, J = 6.9 Hz, 6H); ^{13}C NMR (100 MHz, $CDCl_3$, 298 K):

 This journal is © The Royal Society of Chemistry 2011

Published on 24 March 2011. Downloaded by Nipissing University on 17/10/2014 03:02:48.

δ = 151.83, 141.09, 141.01, 140.05, 139.62, 133.03, 126.26, 125.90, 125.46, 123.55, 123.19, 121.81, 120.64, 120.00, 119.00, 118.97, 109.01, 108.97, 55.44, 43.39, 40.73, 32.10, 31.99, 31.78, 29.87, 29.83, 29.54, 29.44, 29.40, 29.16, 27.17, 22.86, 14.28.

General synthesis of complex

A mixture of 2-ethoxyethanol and water (3 : 1, v/v) was added to a flask containing $IrCl_3 \cdot 3H_2O$ (1 mmol) and the appropriate C^N ligand (2.5 mmol). The mixture was refluxed for 24 h. After cooling, the solid precipitate was filtered to give crude cyclometalated iridium(III) chloro-bridged dimer. The solution of cyclometalated iridium(III) chloro-bridged dimer (0.079 mmol) and the appropriate N^N ligand (0.158 mmol) in CH_2Cl_2–MeOH [30 mL, 2 : 1 (v/v)] was heated to reflux. After 4 h, the solution was cooled to room temperature and then a 10-fold excess of potassium hexafluorophosphate was added. The suspension was stirred for 2 h and then was filtered to remove insoluble inorganic salts. The solution was evaporated to dryness under reduced pressure. It was chromatographed by using CH_2Cl_2/acetone (50 : 1) to afford the solid in 70% yield.

Complex 1. ^{1}H NMR (400 MHz, $CDCl_3$, 298 K): δ = 8.44 (d, J = 4.72 Hz, 2H), 8.22 (t, J = 7.69 Hz, 3H), 8.12–8.08 (m, 2H), 7.90–7.64 (m, 14H), 7.55–7.35 (m, 12H), 7.30–7.26 (m, 3H), 7.21–7.10 (m, 6H), 6.70–6.82 (m, 2H), 6.73–6.63 (m, 2H), 6.48 (s, 4H), 6.36 (s, 4H), 4.36–4.28 (m, 6H), 2.24 (s, 6H), 2.13 (s, 6H), 1.97–1.86 (m, 8H), 1.60 (s, 12H), 1.57(s, 12H), 1.47–1.26 (m, 19H), 1.21–1.10 (m, 13H), 0.88 (t, J = 6.91 Hz, 9H); ^{13}C NMR (100 MHz, $CDCl_3$, 298 K): δ = 169.67, 169.27, 151.83, 151.74, 151.36, 151.03, 149.65, 148.72, 148.53, 147.55, 147.26, 147.05, 146.78, 141.12, 141.08, 140.88, 140.22, 140.15, 139.53, 138.81, 138.11, 137.99, 137.88, 136.30, 132.55, 132.44, 128.61, 127.79, 127.69, 127.42, 126.75, 125.94, 125.63, 125.35, 124.95, 124.64, 124.14, 123.62, 123.07, 121.70, 120.59, 120.01, 119.11, 118.79, 117.96, 117.18, 116.51, 111.87, 109.28, 109.10, 55.38, 45.50, 43.39, 40.86, 40.51, 32.06, 31.94, 31.75, 31.71, 30.14, 29.83, 29.79, 29.69, 29.49, 29.38, 29.15, 29.12, 27.14, 27.10, 25.53, 24.09, 23.93, 22.95, 22.73, 22.70, 22.66, 21.42, 21.32, 14.17, 14.14; MS (MALDI-TOF) [m/z]: 1097.632 (**1** − CzfpbiCz-PF_6)$^+$.

Complex 2. ^{1}H NMR (400 MHz, $CDCl_3$, 298 K): δ = 8.43 (d, J = 9.8 Hz, 2H), 8.17–8.05 (m, 7H), 7.98 (d, J = 7.8 Hz, 1H), 7.88–7.75 (m, 8H), 7.66–7.43 (m, 11H), 7.35–6.88 (m, 12H), 6.78–6.70 (m, 4H), 6.49–6.57 (m, 2H),6.30 (d, J = 8.4 Hz, 1H), 4.18–4.61 (m, 6H), 2.13–1.86 (m, 9H), 1.43–1.12 (m, 32H), 0.87 (t, J = 7.1 Hz, 6H), 0.79 (t, J = 6.9 Hz, 3H); ^{13}C NMR (100 MHz, $CDCl_3$, 298 K): δ = 170.38, 169.68, 154.44, 151.93, 151.81, 151.14, 147.62, 147.25, 147.00, 146.72, 145.61, 141.16, 141.12, 141.06, 141.01, 140.15, 140.12, 137.62, 136.17, 132.55, 132.50, 130.96, 130.73, 130.54, 127.55, 127.42, 127.33, 126.95, 126.08, 125.34, 125.32, 123.61, 123.55, 123.08, 123.02, 120.08, 119.15, 119.11, 118.84, 118.78, 117.38, 116.50, 109.28, 109.08, 43.41, 31.95, 31.74, 31.71, 30.15, 29.83, 29.39, 29.36, 29.16, 29.11, 27.14, 27.10, 22.74, 22.68, 22.66, 14.17, 14.15; MS (ESI-MS) [m/z]: 1655.00 (**2** − PF_6)$^+$.

Complex A1. ^{1}H NMR (400 MHz, $CDCl_3$, 298 K): δ = 8.33–8.18 (m, 3H), 7.98–7.93 (m, 2H), 7.83 (d, J = 7.9 Hz, 1H), 7.76–7.70 (m, 4H), 7.58 (d, J = 8.1 Hz, 1H), 7.58 (d, J = 8.1 Hz, 1H), 7.39–7.23 (m, 7H), 7.06–6.94 (m, 3H), 6.74 (t, J = 7.4 Hz, 1H), 6.60 (d, J = 8.3 Hz, 1H), 6.50–6.48 (m, J = 8.0 Hz, 8H), 6.34 (s, 1H), 6.28 (s, 1H), 4.69–4.45 (m, 2H), 2.24 (d, J = 13.6 Hz, 12H), 2.24 (s, 24H), 1.06–0.81 (m, 8H), 0.73 (t, J = 6.9 Hz, 3H); ^{13}C NMR (100 MHz, $CDCl_3$, 298 K): δ = 168.97, 168.39, 150.54, 150.05, 148.56, 147.96, 147.65, 146.91, 146.48, 146.22, 146.20, 146.13, 140.71, 140.53, 139.57, 139.29, 139.25, 138.44, 137.88, 137.53, 137.06, 137.01, 135.28, 129.79, 129.24, 128.89, 127.78, 127.73, 126.80, 126.73, 126.64, 125.73, 125.55, 125.10, 124.60, 124.52, 124.36, 124.11, 123.91, 123.41, 117.09, 116.30, 115.77, 110.89, 44.83, 30.24, 28.83, 24.79, 21.35, 20.43, 20.38, 13.25; MS (ESI-MS) [m/z]: 1376.50 (**A1** − PF_6)$^+$.

Complex A2. ^{1}H NMR (400 MHz, $CDCl_3$, 298 K): δ = 8.22–8.14 (m, 5H), 8.03 (d, J = 7.2 Hz, 1H), 7.96 (dd, J = 8.8 Hz, 3.3 Hz, 1H), 7.87 (dd, J = 8.0 Hz, 4.2, 1H), 7.72 (dd, J = 8.1 Hz, 1.1 Hz, 1H), 7.60 (d, J = 7.0 Hz, 1H), 7.41–7.27(m, 5H), 7.16–7.06 (m, 4H), 6.95 (ddd, J = 8.7 Hz, 6.9 Hz, 1.4 Hz, 1H), 6.87–6.80 (m, 3H), 6.60 (dd, J = 7.1 Hz, 3.9 Hz, 2H), 6.49 (d, J = 8.4 Hz, 1H), 4.58–4.30 (m, 2H), 1.38–0.91 (m, 8H), 0.76 (t, J = 7.1 Hz, 3H); ^{13}C NMR (100 MHz, $CDCl_3$, 298 K): δ = 170.77, 169.97, 151.84, 151.37, 148.71, 147.79, 147.61, 147.23, 147.08, 147.02, 145.71, 140.51, 140.06, 139.32, 137.99, 136.10, 134.82, 134.56, 131.09, 130.91, 130.83, 129.01, 127.68, 127.61, 127.56, 127.07, 126.94, 126.68, 126.41, 126.16, 126.07, 125.20, 125.03, 124.68, 123.05, 122.96, 118.10, 117.55, 116.77, 111.78, 45.67, 31.26, 29.48, 25.76, 22.39, 14.25; MS (ESI-MS) [m/z]: 880.17 (**A2** − PF_6)$^+$.

Results and discussion

Synthesis and characterization of complex 1 and reference compounds

Scheme 2 shows the synthetic route to complex **1** and reference compounds CzFCz, **2**, **A1** and **A2**. It includes four steps. The first is the synthesis of cyclometalated C^N ligand (Rpq). Ligand **L2** and precursor 2-(4-bromophenyl)quinoline (Brpq) were easily obtained in good yield by a Friedländer condensation reaction.[10] Then, ligand **L1** (Bpq) was synthesized in about 60% yield by lithiating Brpq, followed by the addition of dimesitylboron fluoride (Mes_2BF) at −78 °C.[6c] The second step is the synthesis of N^N ligand CzfpbiCz and Pbi-C_6. Pbi-C_6 was synthesized by *N*-alkylation reaction from 2-(pyridin-2-yl)benzimidazole. The oligomeric N^N ligand CzfpbiCz was obtained by Suzuki coupling reaction from BrfpbiBr and 9-hexylcarbazole-3-boronic acid.[11,14] And the donor compound CzFCz was also synthesized by a similar Suzuki coupling reaction. In order to obtain the target complex **1** and other reference complexes, the dinuclear cyclometalated Ir(III) chloro-bridged precursor $[Ir(Rpq)_2Cl]_2$ with Rpq as cyclometalated ligand was synthesized firstly using the same method as that reported by Nonoyama.[15] Finally the cationic Ir(III) complexes were routinely synthesized with high yields of about 70% by reacting cyclometalated Ir(III) chloro-bridged precursor with the appropriate N^N ligands. The structures of the target complex and reference complexes were characterized by ^{1}H NMR spectroscopy, ^{13}C NMR spectroscopy, MALDI-TOF-MS spectroscopy and ESI-MS spectroscopy.

Published on 24 March 2011. Downloaded by Nipissing University on 17/10/2014 03:02:48.

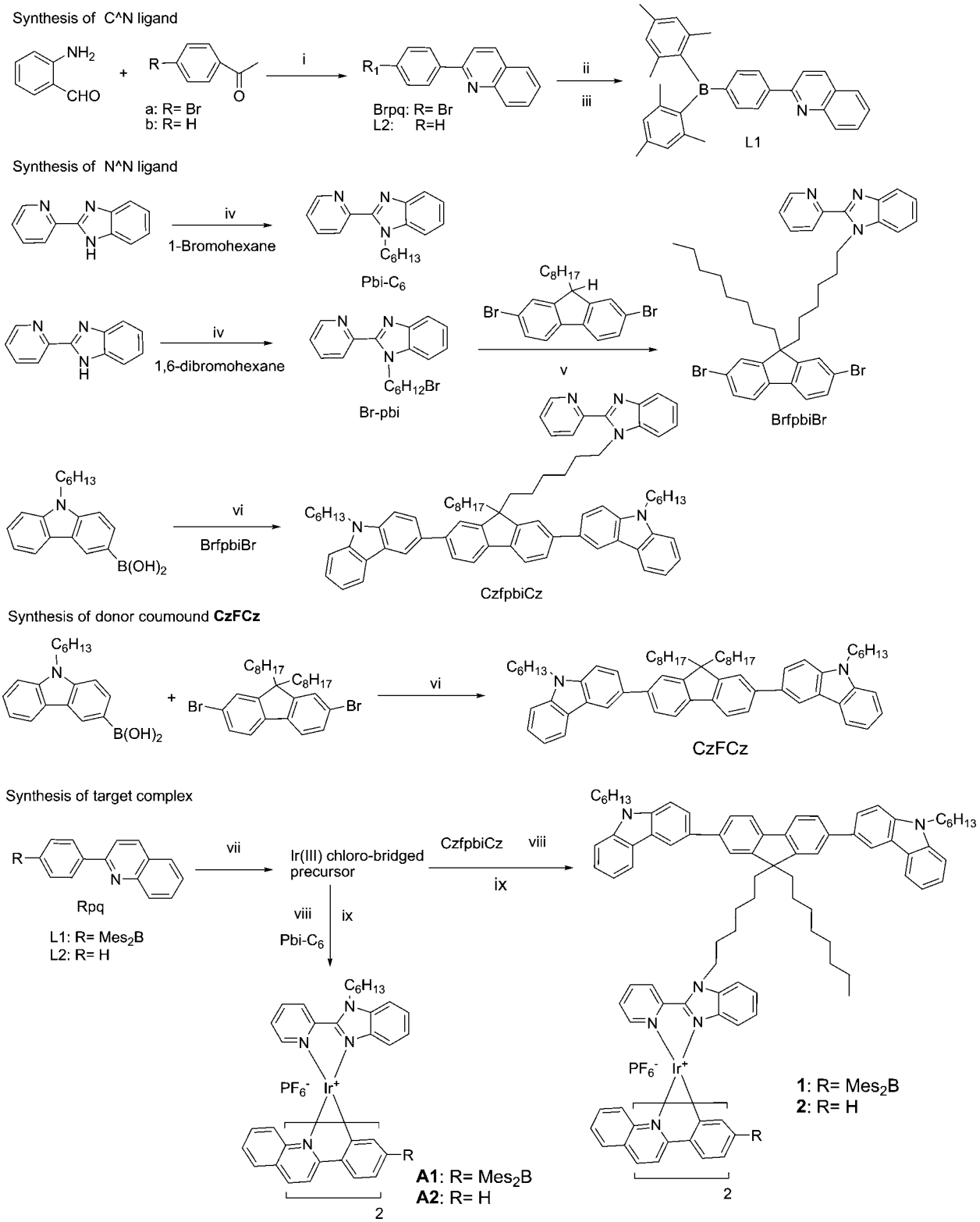

Scheme 2 The synthetic route to the reference compounds and the target complex. *Reagents and conditions*: i) NaOH, EtOH, reflux, overnight; ii) *n*-BuLi, THF, −78 °C, 1 h; iii) Mes_2BF, THF, −78 °C 1h; iv) KOH, [Bmim]BF_4, 20 °C, 5–6 h; v) KOH, DMSO, 60 °C, 6 h; vi) $Pd(PPh_3)_4$, 2 M K_2CO_3 (aq), toluene, EtOH, 70 °C, 24h; vii) $IrCl_3 \cdot H_2O$, 2-ethoxyethanol/H_2O = 3/1, 110 °C, 24 h; viii) CH_2Cl_2–CH_3OH = 2 : 1, 40 °C, 4 h; ix) KPF_6, room temperature, 1 h.

 This journal is © The Royal Society of Chemistry 2011

Published on 24 March 2011. Downloaded by Nipissing University on 17/10/2014 03:02:48.

Photophysical properties

The photophysical properties of complex **1** and reference compounds were investigated through UV-vis absorption and photoluminescence (PL) spectroscopy in order to clarify the FRET from the fluorescent donor to the phosphorescent acceptor and the influence of the Mes_2B group on the photophysical properties of the complex.

1) Absorption spectra. The absorption spectra of the complexes (**1**, **2**, **A1** and **A2**) and the normalized PL spectrum of CzFCz are shown in Fig. 2, and the data are summarized in Table 1. From Fig. 2, we can see that the absorption spectrum of **1** can be regarded as the spectral sum of CzFCz and **A1**, indicating weak ground state interaction between them. **1** shows two intense absorption bands centered at $\lambda = 300$ and 345 nm with molar extinction coefficients (ε) of $\sim 10^4$ and weak absorption at $\lambda = 400$–550 nm with ε of $\sim 10^3$ in CH_2Cl_2 solution. The intense absorption bands below $\lambda = 400$ nm are related to the singlet ligand-centered π–π^* transitions from the cyclometalated C^N ligand (Bpq) and N^N ligand of the Ir(III) complex and donor CzFCz. The weak absorption at $\lambda = 400$–550 nm can be assigned to a mixture of spin-allowed ligand-to-ligand charge transfer (LLCT) transition, metal-to-ligand charge transfer (MLCT) transition and spin-forbidden ligand-centered ^{3}LC and ^{3}MLCT transitions.[16] Comparing the spectra of compounds containing Mes_2B (**1** and **A1**) to those without Mes_2B (**2** and **A2**), we can find that the introduction of Mes_2B groups results in significantly red-shifted and more intense absorption. This may be assigned to the enhanced p_π–π^* conjugation between the vacant p orbital of the boron atom and the π conjugated skeleton.

2) Photoluminescence spectra. From Fig. 3, we can see that **1** shows an intense emission band at $\lambda = 584$ nm in CH_2Cl_2 solution with emission lifetime of 2.81 μs and quantum efficiency of 1.1 relative to Φ [*fac*-Ir(ppy)$_3$] = 1. The emission band is similar to that of **A1**, and so can be assigned to emission from the phosphorescent acceptor in **1**. The high quantum efficiency can be assigned to the effects of the Mes_2B unit and FRET. Besides, very weak emission bands at around $\lambda = 419$ nm were also observed, which were similar to those from fluorescent donor CzFCz (see Fig. 3). These results indicate that efficient FRET from the fluorescent donor to the phosphorescent acceptor takes place. The reference complex **2** without Mes_2B groups shows an intense emission at 554 nm from the Ir(III) complex unit, and the obvious blue emission from CzFCz was also observed, indicating less efficient FRET from the donor to the acceptor compared to complex **1**. Hence, the introduction of Mes_2B groups into the C^N ligands results in the red-shift of the Ir(III) complex emission and more efficient FRET from the fluorescent donor to the phosphorescent acceptor.

The photoluminescence spectra of **1** under different conditions were also measured and are shown in Fig. 4. The emission of **1** has little dependence on the solvent polarity and temperature. At 77 K, almost no donor emission was observed, indicating more efficient FRET at low temperature. According to previous studies, the emission from the ligand-centered ^{3}LC(π–π^*) state often displays vibronic progressions and little dependence on solvent polarity and temperature, while those from CT states are often broad, featureless, and sensitive to solvent polarity and temperature.[17] The emission peaks of **1** show little dependence on solvent polarity and temperature (see Fig. 4), indicating that the

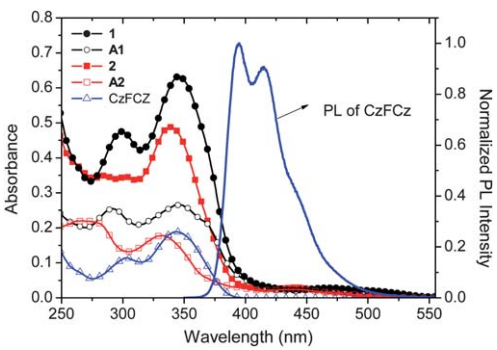

Fig. 2 The absorption spectra of **1**, **2**, **A1**, **A2** and CzFCz and the PL spectrum of CzFCz measured in CH_2Cl_2 solution.

Table 1 Photophysical data

Compound	λ_{abs}/nm (logε)	λ_{em}/nm (CH_2Cl_2)
1	300 (4.98), 345 (5.10), 460 (3.75)	584
2	338 (4.99), 440 (3.76)	394, 415, 554
A1	291 (4.71), 345 (4.72), 460 (3.70)	584
A2	272 (4.64), 332 (4.55), 440 (3.70)	554
CzFCz	303 (4.36), 344 (4.58)	394, 415

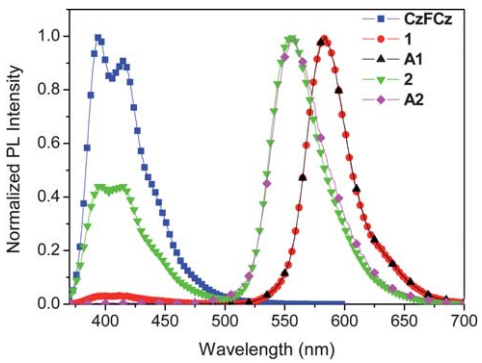

Fig. 3 The normalized photoluminescence spectra of CzFCz, **1**, **2**, **A1** and **A2** measured in CH_2Cl_2 solution.

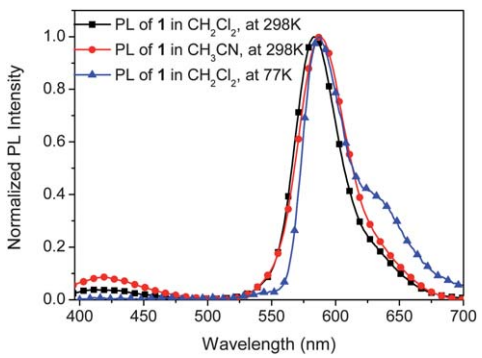

Fig. 4 The normalized photoluminescence spectra of probe **1** measured under different conditions.

Published on 24 March 2011. Downloaded by Nipissing University on 17/10/2014 03:02:48.

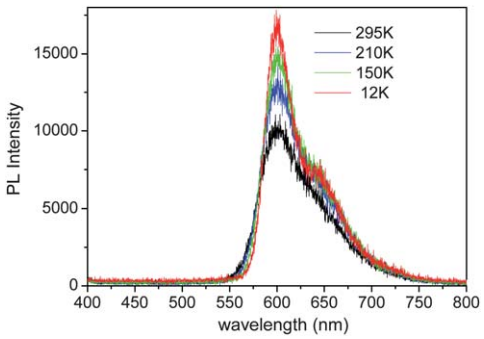

Fig. 5 Temperature dependence of PL spectra of **1** in neat films spin-coated on quartz plates.

^{3}LC state dominates the excited states. In addition, no vibronic progressions were observed, indicating that the excited state of the complex is complicated and has some CT character.

The emission properties of **1** in film was also investigated. The emission band in film is red-shifted to 600 nm with a shoulder at 650 nm (see Fig. 5). No emission from the fluorescent donor was observed, indicating more efficient FRET in film than in solution. And the quantum efficiency for **1** in film was measured to be 0.15 under excitation at $\lambda = 450$ nm. The dependence of solid-film emission spectra for **1** on temperature was also studied (see Fig. 5). With the decrease of temperature from 295 K to 12 K, no evident shift of emission wavelength was observed. However, it is noteworthy that the emission intensity was enhanced significantly, indicating the reduced non-radiative channels for excited states at low temperature.

3) FRET from fluorescent donor to phosphorescent acceptor. From the results obtained above, we can see that the introduction of Mes_2B groups into the complex can improve the efficiency of FRET from the fluorescent donor to the phosphorescent acceptor significantly. The efficiency of FRET depends on the spectral overlap between the emission spectrum of the donor and the absorption spectrum of the acceptor. In order to clarify the different efficiencies of FRET for **1** and **2**, the overlap between the absorption spectra of phosphorescent guests **A1** or **A2** and the PL spectrum of fluorescent donor CzFCz was compared. From Fig. 2 we can see that the absorption spectrum of **A1** has better overlap with the emission spectrum of CzFCz than **A2** does, which can explain the more efficient FRET observed for complex **1**. The better spectral overlap for **A1** can be assigned to the red-shifted and more intense absorption bands induced by the introduction of Mes_2B groups. Hence, we can see that the introduction of Mes_2B groups will be an effective way to design excellent optoelectronic materials utilizing efficient intramolecular FRET.

Optical responses of 1 to F^-

It has been demonstrated that the vacant p orbital on the boron atom in triarylborane derivative coordinates selectively with fluoride anions, giving rise to changes in both absorption and emission spectra.[7] In the present study, the ability of probe **1** to complex with F^- was investigated using UV-vis absorption and emission titration experiments.

From Fig. 6, we can see that the absorbances at $\lambda = 300$ and 345 nm decreased gradually upon addition of F^- to **1** in CH_2Cl_2 solution. In addition, the absorbances in the range of $\lambda = 400$–550 nm increased slightly. An obvious isosbestic point at $\lambda = 383$ nm was observed. To quantify the F^- concentration in solution, the change in absorption spectra (see Fig. 6) is correlated to the analyte concentration using $f = (A_0 - A)/A_0$, where A and A_0 are the absorbances at $\lambda = 345$ nm in the presence and absence of F^-, respectively. The calibration factor (f) is defined to minimize the influence of the absorption background in the absence of F^-. Fig. 7 shows f as a function of F^- concentration in CH_2Cl_2 solution. From Fig. 7, we can see that **1** gives a linear response to F^- in the range 0–50 μM and the correlation coefficient is 0.99, which is suitable for F^- monitoring and quantification in the range 0–50 μM. Furthermore, using the UV-vis titration data, the binding constants K_1 and K_2 of probe **1** were determined to be 8.31×10^5 and 9.00×10^3 M^{-1}, respectively (see Fig. S3†).

The response of probe **1** to F^- was further investigated by PL spectroscopy with $\lambda = 383$ nm (isobestic point) as the excitation wavelength (shown in Fig. 8). Upon addition of F^- to **1**, the emission intensity at $\lambda = 584$ nm assigned to the phosphorescent acceptor decreased accompanied by a blue-shift to $\lambda = 554$ nm gradually, whereas the emission intensity at $\lambda = 392$–419 nm assigned to the fluorescence donor (CzFCz) increased

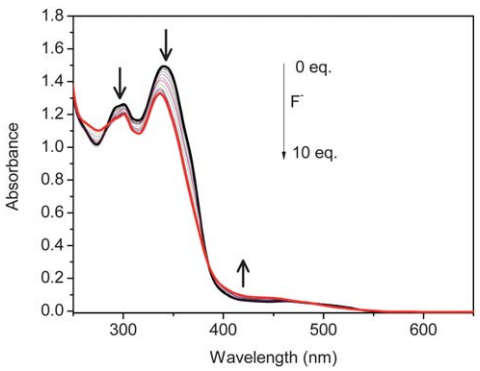

Fig. 6 Change in the UV-vis absorption spectra of **1** (20 μM) in CH_2Cl_2 solution with various amounts of F^-.

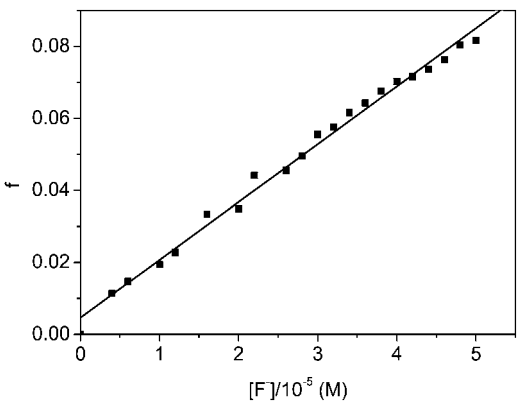

Fig. 7 f as a function of F^- concentration for **1** (20 μM) in CH_2Cl_2 solution at room temperature. ($f = (A_0 - A)/A_0$, where A and A_0 are the absorbances at $\lambda = 345$ nm in the presence and absence of F^-, respectively, and the correlation coefficient is 0.99).

 This journal is © The Royal Society of Chemistry 2011

Published on 24 March 2011. Downloaded by Nipissing University on 17/10/2014 03:02:48.

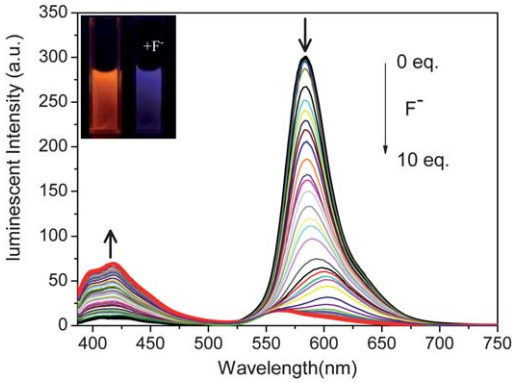

Fig. 8 Change in the PL spectra of **1** (20 μM) in a CH_2Cl_2 solution with various amounts of F^-. λ_{ex} = 383 nm. Inset: emission color observed in a CH_2Cl_2 solution of **1** (20 μM) in the absence (left) and presence (right) of 10 equiv. F^-.

simultaneously, realizing the ratiometric detection for F^-. Such ratiometric detection can be assigned to the changed FRET efficiency from the donor to th eacceptor induced by the binding of F^-.[7e] The ratios of emission intensities at λ = 584 and 419 nm (I_{584nm}/I_{419nm}) exhibit a dramatic change from 33.0 to 0.4. Such a large change of emission intensity ratios at two wavelengths is desirable for ratiometric fluorescent probes, as the sensitivity as well as the dynamic range of ratiometric probes are controlled by the emission ratio. Furthermore, the difference in two emission wavelengths is very large (165 nm). This difference not only contributes to the accurate measurement of two emission intensities, but also results in a huge ratiometric value. More importantly, the emission color of solution was changed from orange-red to blue, realizing naked-eye detection (Fig. 8, inset). Hence, excellent ratiometric and colorimetric F^- detection was realized.

As shown by the emission titration curves (Fig. 9), probe **1** needs approximately 2 equivalents of F^- to reach saturation point. Considering that there are two boron centers in one probe molecule, it is possible for **1** to form a 1 : 2 complex with 2 equivalents of F^- because the two Mes_2B groups are electronically separated in the ground state and spatially distant from each other.

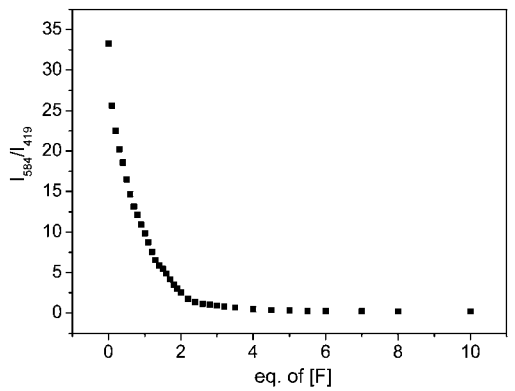

Fig. 9 Fluorescent titration curve of the ratio of emission intensity at λ = 584 nm and λ = 419 nm (I_{584nm}/I_{419nm}) *versus* the number of equivalents of F^-.

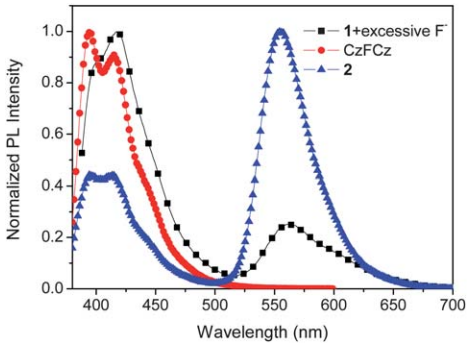

Fig. 10 The normalized PL spectra of **1** with excess F^-, CzFCz and **2**.

Fig. 10 shows the normalized PL intensity of **1** with excess F^- along with CzFCz and **2**. The complex **1**-2F^- shows a phosphorescent emission peak at 554 nm, which is similar to the phosphorescent emission of **2** and **A2**. This indicates that the complexation of the Mes_2B group with F^- interrupts the conjugation of the p orbital of the boron atom with the π conjugated skeleton. In addition, the blue emission at λ = 390–419 nm for **1**-2F^- is similar to that of donor CzFCz. Although the emission bands of complex **1**-2F^- are similar to those of **2** without Mes_2B groups, the intensity ratio of blue fluorescence to orange phosphorescence is obviously increased compared with that of **2**. This is because the complexation of **1** with F^- quenches the emission from the Ir(III) complex unit partly and affects the FRET from the donor to the acceptor.

High selectivity is necessary for an excellent probe. Herein, the selective binding studies of probe **1** were then extended to other anions in CH_2Cl_2 solution. As shown in Fig. 11, only the addition of F^- results in a prominent change of I_{584nm}/I_{419nm}, whereas the addition of other anions (Cl^-, Br^-, I^-, ClO_4^-, NO_3^-, $H_2PO_4^-$, CH_3COO^-) causes little changes. Therefore, probe **1** displayed a high selectivity in sensing F^-. Similarly, achieving high selectivity for the analyte of interest over a complex background of potentially competing species is a challenge in probe development. Thus, the competition experiment was also carried out by adding F^- to solutions of **1** in the presence of other anions. As shown in Fig. 11, whether in the absence or presence of other anions, obvious spectral changes were observed for **1** upon addition of F^-, indicating that the sensing of F^- by **1** is hardly affected by other anions.

Sensing mechanism of 1

In order to better understand the excited state properties and sensing mechanism of probe **1**, molecular orbital calculations for a model complex (**1′**) of **1** without donor CzFCz and the adduct **1′-2F**$^-$ were performed using DFT and time-dependent density functional theory (TDDFT) calculations (see Fig. 12, Fig. 13 and Table 2). For **1′**, the lowest triplet state (T_1) originates from HOMO → LUMO (43%) and HOMO → LUMO + 2 (45%). The HOMO distribution primarily resides on the phenyl of the cyclometalated ligands and the Ir(III) center. The LUMO distribution is dominated by the 2-(pyridin-2-yl)benzimidazole (pbi) fragment, and the LUMO + 2 distribution primarily resides on the Bpq. Hence, the lowest triplet state apparently possesses

Published on 24 March 2011. Downloaded by Nipissing University on 17/10/2014 03:02:48.

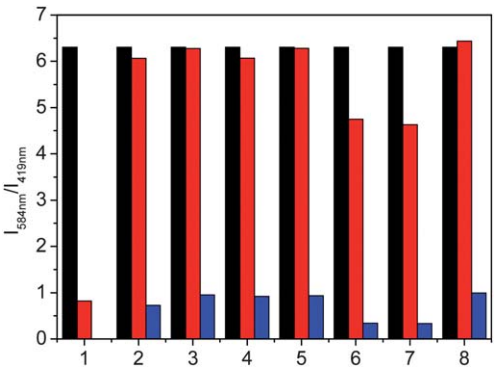

Fig. 11 Emission response of probe **1** (20 μM) in the presence of various anions (4 equiv) in CH_2Cl_2 solution. Bars represent the ratio of emission intensity at $\lambda = 584$ nm and $\lambda = 419$ nm (I_{584nm}/I_{419nm}). Black and red represent I_{584nm}/I_{419nm} before and after the addition of anions, respectively. Blue bar represents I_{584nm}/I_{419nm} after addition of F^- to the solution of **1** containing other anions. 1, F^-; 2, Cl^-; 3, Br^-; 4, I^-; 5, NO_3^-; 6, $H_2PO_4^-$; 7, CH_3COO^-; 8, ClO_4^-.

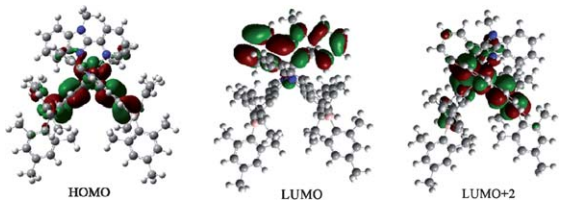

Fig. 12 Calculated orbital distributions of **1′**.

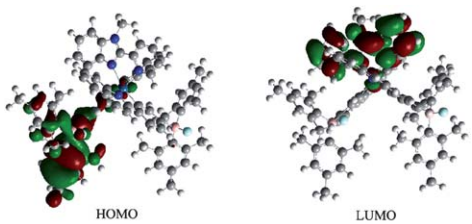

Fig. 13 Calculated orbital distributions of **1′-2F⁻**.

ligand-centered (C^N ligand) character (^{3}LC), which mixes with [$\pi_{phenyl} \rightarrow \pi^*_{N^N}$] (^{3}LLCT), and [d$\pi$(Ir center) $\rightarrow \pi^*_{N^N}$] (^{3}MLCT) transitions. This is in accordance with the emission character, which apparently possesses a mixture of ^{3}LC and CT transitions. Such complicated excited states lead to the intense phosphorescent emission at $\lambda = 584$ nm. After binding with F^-, the T_1 of **1′-F⁻** mainly originates from the HOMO → LUMO transition. The HOMO distributions primarily reside on the Mes_2B–F^- fragment, and the LUMO distribution resides on the pbi fragment. So, the T_1 of **1′-2F⁻** can be assigned to the ^{3}LLCT transition from the Mes_2B group to the N^N ligand. We tentatively think that the formation of this transition is responsible for the quenching of the original emission at 584 nm and the final emission band at 554 nm of the adduct **1-2F⁻** is assigned to the emission from **A2** without Mes_2B groups.

Hence, according to the spectral properties, emission titration experiment and theoretical calculation results, we can summarize the sensing mechanism as follows. Before binding with F^-, there

Table 2 Calculated lowest triplet states for **1′** and **1′-2F⁻**

	State	Excitation
1′	T_1	HOMO → LUMO (43%) HOMO → LUMO + 2 (45%)
1′-2F⁻	T_1	HOMO → LUMO (69%)

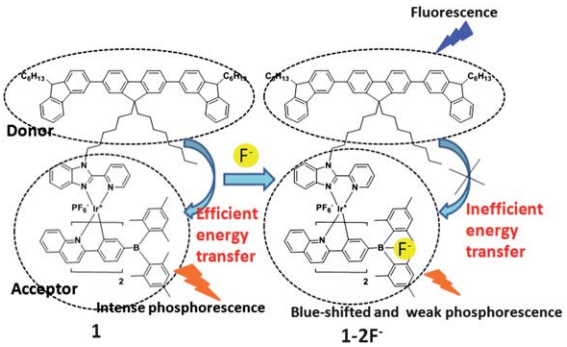

Fig. 14 The sensing mechanism of probe **1**.

is efficient FRET from the donor to the acceptor, leading to the intense phosphorescent emission from the Ir(III) complex unit. However, the binding of F^- can cause the significant variations in photophysical properties of the Ir(III) complex unit and subsequent FRET efficiency between the donor and the acceptor, leading to the restored blue fluorescence from the donor CzFCz (see Fig. 14).

Conclusion

In summary, a FRET-based F^- probe (**1**) based on carbazole-fluorene-carbazole as the fluorescent donor and a Mes_2B group-functionalized cationic Ir(III) complex as the phosphorescent acceptor has been designed and synthesized. Compared with the reference compounds, the introduction of Mes_2B groups on the ligands of the Ir(III) complex unit can lead to red-shifted and more intense absorption and phosphorescence emission. In addition, the FRET efficiency from the fluorescent donor to the phosphorescent acceptor can be enhanced significantly. The binding of probe **1** with F^- changes the excited-state properties of the Ir(III) complex unit and suppresses the FRET from the donor to the acceptor, enhancing the blue emission from the fluorescent donor. So, this complex can be used as a highly selective, colorimetric and ratiometric phosphorescent probe for F^- utilizing the switchable phosphorescence and fluorescence. This work may be very useful for the further design of excellent ratiometric and colorimetric probes utilizing switchable phosphorescent and fluorescent emissions.

Acknowledgements

This work was financially supported by the National Basic Research Program of China (973 Program, 2009CB930601), National Natural Science Foundation of China (Project No. 50803028 and 20804019), Natural Science Foundation of Jiangsu Province of China (BK2009427), Natural science fund for colleges and universities in Jiangsu Province (10KJB430010),

 This journal is © The Royal Society of Chemistry 2011

scientific and technological innovation teams of colleges and universities in Jiangsu Province (TJ209035), Scientific and Technological Activities for Returned Personnel in Nanjing City (NJ209001), Nanjing University of Posts and Telecommunications (Project No. NY210029), and the Program for Postgraduates Research Innovations in University of Jiangsu Province (CX08B_084Z).

Published on 24 March 2011. Downloaded by Nipissing University on 17/10/2014 03:02:48.

Notes and references

1 K. L. Kirk, *Biochemistry of the Halogens and Inorganic Halides*, Plenum Press, New York, 1991, p. 58.

2 (*a*) B. L. Riggs, *Bone and Mineral Research, Annual 2*, Elsevier, Amsterdam, The Netherlands, 1984, p. 366; (*b*) D. G. Cho and J. L. Sessler, *Chem. Soc. Rev.*, 2009, **38**, 1647; (*c*) M. Cametti and K. Rissanen, *Chem. Commun.*, 2009, 2809; (*d*) K. Parab, K. Venkatasubbaiah and F. Jäkle, *J. Am. Chem. Soc.*, 2006, **128**, 12879; (*e*) S. Yamaguchi, S. Akiyama and K. Tamao, *J. Am. Chem. Soc.*, 2001, **123**, 11372.

3 (*a*) P. D. Beer and P. A. Gale, *Angew. Chem., Int. Ed.*, 2001, **40**, 486; (*b*) H. Miyaji, W. Sato and J. L. Sessler, *Angew. Chem., Int. Ed.*, 2000, **39**, 1777; (*c*) C. B. Black, B. Andrioletti, A. C. Try, C. Ruiperez and J. L. Sessler, *J. Am. Chem. Soc.*, 1999, **121**, 10438; (*d*) E. J. Cho, J. W. Moon, S. W. Ko, J. Y. Lee, S. K. Kim, J. Yoon and K. C. Nam, *J. Am. Chem. Soc.*, 2003, **125**, 12376; (*e*) M. Boiocchi, L. D. Boca, D. E. Gomez, L. Fabbrizzi, M. Licchelli and E. Monzani, *J. Am. Chem. Soc.*, 2004, **126**, 16507; (*f*) K. Chellappan, N. J. Singh, I. C. Hwang, J. W. Lee and K. S. Kim, *Angew. Chem., Int. Ed.*, 2005, **44**, 2899.

4 (*a*) Z. Q. Liu, M. Shi, F. Y. Li, Q. Fang, Z. H. Chen, T. Yi and C. H. Huang, *Org. Lett.*, 2005, **7**, 5481; (*b*) M. H. Lee, T. Agou, J. Kobayashi, T. Kawashima and F. P. Gabbaï, *Chem. Commun.*, 2007, 1133; (*c*) X. Y. Liu, D. R. Bai and S. Wang, *Angew. Chem., Int. Ed.*, 2006, **45**, 5475; (*d*) D. R. Bai, X. Y. Liu and S. Wang, *Chem.–Eur. J.*, 2007, **13**, 5713.

5 (*a*) T. W. Hudnall and F. P. Gabbaï, *J. Am. Chem. Soc.*, 2007, **129**, 11978; (*b*) Y. M. You and S. Y. Park, *Adv. Mater.*, 2008, **20**, 3820; (*c*) E. Sakuda, A. Funahashi and N. Kitamura, *Inorg. Chem.*, 2006, **45**, 10670; (*d*) Q. Zhao, F. Y. Li and C. H. Huang, *Chem. Soc. Rev.*, 2010, **39**, 3007; (*e*) Q. Zhao, F. Y. Li and C. H. Huang, *Chem. Soc. Rev.*, 2011, DOI: 10.1039/C0CS00114G.

6 (*a*) Q. Zhao, T. Y. Cao, F. Y. Li, X. H. Li, H. Jing, T. Yi and C. H. Huang, *Organometallics*, 2007, **26**, 2077; (*b*) Q. Zhao, S. J. Liu, F. Y. Li, T. Yi and C. H. Huang, *Dalton Trans.*, 2008, 3836; (*c*) Q. Zhao, F. Y. Li, S. J. Liu, M. X. Yu, Z. Q. Liu, T. Yi and C. H. Huang, *Inorg. Chem.*, 2008, **47**, 9256; (*d*) H. L. Chen, Q. Zhao, F. Y. Li, Y. B. Wu, H. Yang, T. Yi and C. H. Huang, *Inorg. Chem.*, 2007, **46**, 11075; (*e*) W. J. Xu, S. J. Liu, X. Y. Zhao, S. Sun, S. Cheng, T. C. Ma, H. B. Sun, Q. Zhao and W. Huang, *Chem. Eur. J.*, 2010, **16**, 7125; (*f*) H. F. Shi, S. J. Liu, H. B. Sun, W. J. Xu, Z. F. An, J. Chen, S. Sun, X. M. Lu, Q. Zhao and W. Huang, *Chem.–Eur. J.*, 2010, **16**, 12158; (*g*) Q. Zhao, M. X. Yu, L. X. Shi, S. J. Liu, C. Y. Li, M. Shi, Z. G. Zhou, C. H. Huang and F. Y. Li, *Organometallics*, 2010, **29**, 1085; (*h*) L. Q. Xiong, Q. Zhao, H. L. Chen, Y. B. Wu, Z. S. Dong, Z. G. Zhou and F. Y. Li, *Inorg. Chem.*, 2010, **49**, 6402; (*i*) H. Z. Wu, T. S. Yang, Q. Zhao, J. Zhou, C. Y. Lia and F. Y. Li, *Dalton Trans.*, 2011, **40**, 1969.

7 (*a*) S. B. Zhao, T. McCormick and S. Wang, *Inorg. Chem.*, 2007, **46**, 10965; (*b*) Y. Sun, N. Ross, S. B. Zhao, K. Huszarik, W. L. Jia, R. Y. Wang, D. Macartney and S. Wang, *J. Am. Chem. Soc.*, 2007, **129**, 7510; (*c*) S. T. Lam, N. Y. Zhu and V. W. W. Yam, *Inorg. Chem.*, 2009, **48**, 9664; (*d*) Y. L. Rao and S. Wang, *Inorg. Chem.*, 2009, **48**, 7698; (*e*) Z. M. Hudson, S. B. Zhao, R. Y. Wang and S. Wang, *Chem.–Eur. J.*, 2009, **15**, 6131; (*f*) Y. Sun and S. Wang, *Inorg. Chem.*, 2009, **48**, 3755.

8 (*a*) Y. Kubo, M. Yamamoto, M. Ikeda, M. Takeuchi, S. Shinkai, S. Yamaguchi and K. Tamao, *Angew. Chem., Int. Ed.*, 2003, **42**, 2036; (*b*) S. Maruyama, K. Kikuchi, T. Hirano, Y. Urano and T. Nagano, *J. Am. Chem. Soc.*, 2002, **124**, 10650; (*c*) F. WKrthner, S. Ahmed, C. Thalacker and T. Debaerdemaeker, *Chem.–Eur. J.*, 2002, **8**, 4742; (*d*) Z. G. Zhou, M. X. Yu, H. Yang, K. W. Huang, F. Y. Li, T. Yi and C. H. Huang, *Chem. Commun.*, 2008, 3387.

9 M. J. Frisch, G. W. Trucks, H. B. Schlegel, G. E. Scuseria, M. A. Robb, J. R. Cheeseman, J. A. Montgomery, T. Vreven, K. N. Kudin, J. C. Burant, J. M. Millam, S. S. Iyengar, J. Tomasi, V. Barone, B. Mennucci, M. Cossi, G. Scalmani, N. Rega, G. A. Petersson, H. Nakatsuji, M. Hada, M. Ehara, K. Toyota, R. Fukuda, J. Hasegawa, M. Ishida, T. Nakajima, Y. Honda, O. Kitao, H. Nakai, M. Klene, X. Li, J. E. Knox, H. P. Hratchian, J. B. Cross, V. Bakken, C. Adamo, J. Jaramillo, R. Gomperts, R. E. Stratmann, O. Yazyev, A. J. Austin, R. Cammi, C. Pomelli, J. W. Ochterski, P. Y. Ayala, K. Morokuma, G. A. Voth, P. Salvador, J. J. Dannenberg, V. G. Zakrzewski, S. Dapprich, A. D. Daniels, M. C. Strain, O. Farkas, D. K. Malick, A. D. Rabuck, K. Raghavachari, J. B. Foresman, J. V. Ortiz, Q. Cui, A. G. Baboul, S. Clifford, J. Cioslowski, B. B. Stefanov, G. Liu, A. Liashenko, P. Piskorz, I. Komaromi, R. L. Martin, D. J. Fox, T. Keith, M. A. Al-Laham, C. Y. Peng, A. Nanayakkara, M. Challacombe, P. M. W. Gill, B. Johnson, W. Chen, M. W. Wong, C. Gonzalez and J. A. Pople, *Gaussian 03, revision C.02*; Gaussian, Inc., Wallingford, CT, 2004.

10 Y. Z. Hu, G. Zhang and R. P. Thummel, *Org. Lett.*, 2003, **5**, 2251.

11 R. Stahl, C. Lambert, C. Kaiser, R. Wortmann and R. Jakober, *Chem.–Eur. J.*, 2006, **12**, 2358.

12 (*a*) H. Y. Wang, G. Chen, Y. Liu, L. H. Hu, X. P. Xu and S. J. Ji, *Dyes Pigm.*, 2009, **83**, 269; (*b*) W. L. Yu, J. Pei, Y. Cao, W. Huang and A. J. Heeger, *Chem. Commun.*, 1999, 1837.

13 Z. G. Le, Z. C. Chen, Y. Hu and Q. G. Zheng, *Synthesis*, 2004, **2**, 208.

14 N. Miyaura and A. Suzuki, *J. Chem. Soc., Chem. Commun.*, 1979, 866.

15 K. Nonoyama, *Bull. Chem. Soc. Jpn.*, 1974, **47**, 767.

16 (*a*) Q. Zhao, S. J. Liu, M. Shi, C. M. Wang, M. X. Yu, L. Li, F. Y. Li, T. Yi and C. H. Huang, *Inorg. Chem.*, 2006, **45**, 6152; (*b*) F. Neve, A. Crispini, S. Campagna and S. Serroni, *Inorg. Chem.*, 1999, **38**, 2250.

17 (*a*) A. Tsuboyama, H. Iwawaki, M. Furugori, T. Mukaide, J. Kamatani, S. Igawa, T. Moriyama, S. Miura, T. Takiguchi, S. Okada, M. Hoshino and K. Ueno, *J. Am. Chem. Soc.*, 2003, **125**, 12971; (*b*) A. B. Tamayo, S. Garon, T. Sajoto, P. I. Djurovich, I. M. Tsyba, R. Bau and M. E. Thompson, *Inorg. Chem.*, 2005, **44**, 8723.